Heliyon 10 (2024) e27254

Contents lists available at ScienceDirect

Heliyon

journal homepage: www.cell.com/heliyon

Research article

Numerical investigation of louver edges effect on the performances of louvered fin compact heat exchanger

Dessalew Shite Feleke [a,b], Muluken Z. Getie [a,*], Temesgen Asefa Minale [a]

[a] Faculty of Mechanical and Industrial Engineering, Bahir Dar Institute of Technology, Bahir Dar University, Bahir Dar, P.O.Box: 26, Amhara, Ethiopia

[b] Department of Mechanical Engineering, Debre Tabor University, Debre Tabor, P.O.Box 272, Amhara, Ethiopia

ARTICLE INFO

Keywords:
Compact heat exchanger
Friction factor
Louver edge effect
Louvered fin
Volume goodness factor

ABSTRACT

The rectangular channel louvered-fin compact heat exchanger (LFCHE) is the most efficient type that has been served in a radiator. However, with this type of heat exchanger, the pressure drop rises by three to four times as the heat transfer increases, which results in decreasing performance. This research is aimed to numerically investigate the louver edges (vertical, inclined, and horizontal) effect on LFCHE performance at different louver angle (θ) with air inlet velocities ranging from 1 to 30 m/s. A total of twelve models are made and simulated. The result revealed that the horizontal edge decreases the pressure drop up to 24.2% with a 1.01% increase in outlet air temperature over the base model (inclined edge). Thus, louver edge has design which results in higher and lower effect on pressure drop and temperature change, respectively. The research investigated the effects of louver edges using different performance evaluation criteria. At 10 m/s ($Re_{lp} = 972.33$) the horizontal edge increases the volume goodness (jf) factor up to 21.49% over the base model. Similarly, the horizontal edged fins resulted in maximum increment of jf-factor by 22% and 25% as compared with inclined edge for louver angles θ of 24 ° (at low Re_{lp}) and 20 ° (at high Re_{lp}), respectively. Generally, the horizontally edged LFCHE is proven to have higher performance in cooling the coolant with a minimum air side pressure drop.

1. Introduction

The air-cooled compact heat exchangers with louver fin are extensively used in vehicles radiators since it is the most efficient and advanced heat transfer fin surface [1–4]. The heat transfer between the louver fin surface and the air is what drives the predominant heat transfer by interrupting or breaking up the flow of air and creating thin boundary layers, which lowers the thermal resistivity and increases the heat dissipation [5–8]. Increasing the heat transfer rate, decreasing the pressure drop, and compacting the volumes are the basic design consideration for increasing the performance of the heat exchanger [9]. In previous decades, the performance data were presented [10–13] with regard to friction f-factor and Colburn j-factor to get a LFCHE with a high j and a low f-factor of the air side.

Numerous studies have demonstrated that louver fins generally perform better at dissipating heat than other types of fins. Habibian et al. [14] numerically investigated the effect of fin shape on the performance of compact finned-tube heat exchangers. The result revealed that compared to a plain fin, a louvered fin increased the pressure drop and heat transfer by 67.7% and 24.6%, respectively.

* Corresponding author.
E-mail address: muluken.zegeye@bdu.edu.et (M.Z. Getie).

https://doi.org/10.1016/j.heliyon.2024.e27254
Received 11 March 2023; Received in revised form 4 December 2023; Accepted 27 February 2024
Available online 3 March 2024

Nomenclature

A_c	Minimum flow cross-sectional area (m^2)
A_t	Total heat transfer area (m^2)
c_p	Specific heat of fluid $(J/Kg^{\circ}C)$
$c_{p,a}$	Specific heat of air $(J/Kg^{\circ}C)$
f	Friction factor
F_d	Fin depth (mm)
F_l	Fin length (mm)
F_p	Fin pitch (mm)
L_l	Louver length (mm)
h	Heat transfer coefficient (W/m^2K)
j	Colburn j-factor
k_f	Thermal conductivity of fluid $(W/m^{\circ}C)$
$\dot{m}$	Mass flow rate (Kg/sec)
Nu	Nusselt number
ΔP	Pressure drop (Pa)
Q	Heat transfer rate (W)
Re_{lp}	Louver pitch-based Reynolds number
t	Fin thickness (mm)
T_{in}	Bulk temperatures at the inlet (K)
T_{out}	Bulk temperatures at the outlet (K)
T_{wall}	Tube wall temperature (K)
T_p	Tube pitch (mm)
u	Inlet air velocity (m/sec)
u_{ava}	Average air velocity through the fluid domain (m/sec)

Greek Symbol

ε	Rate of kinetic energy dissipation
θ	Louver angle (°)z
κ	Turbulence of the kinetic energy
λ	Thermal conductivity of fluid $(W/m^{\circ}C)$
μ	Dynamic viscosity (Ns/m^2)
μ_t	Turbulent dynamic viscosity (Ns/m^2)
ρ	Density of fluid (Kg/m^3)
ρ_a	Density of air (Kg/m^3)
τ	Viscous stress tensor (Pa)
υ	Kinematic viscosity (m^2/sec)

Dodiya et al. [15] proved that a heat exchanger with a louvered fin yielded a 25% enhancement in heat dissipation and a 110% growth in pressure drop when compared to a plate fin. Gorman et al. [16] compared the louvered and plain fins and found that the louver fins were accompanied with a higher pressure drop and heat dissipation over the plain fins. Yadav et al. [17] improved the geometry of louvered fins and a louvered heat exchanger was produced with a 22.56% increase in heat transfer rate over the base design. Despite louver fins having better overall performances than other fins, recent scholars emphasized the need to improve louver fin geometric structure since the performance of the louver fin is greatly influenced by its geometric and flow parameters [18–22].

Tran and Wang [23] discovered a new fin structure and presented a fin configuration with straight-louver. As compared with the same direction (SD) louvered fin, the new fin model boosts the performance by 19.54, 18.31, and 17.52% at fanning powers of 20, 10, and 2 W, respectively. Saleem and Kim [24] studied thermo-hydraulic performance of air side using a numerical approach in the range of Reynolds number subjected to louver pitch (Re_{lp}) from 30 to 500 and louver angle (19 °-31 °). The optimal thermal performance was obtained at low Re_{lp} and louver angle of (19 °). The effects of geometric parameters on pressure drop and heat transfer were studied experimentally and numerically by Ref. [25]. From the investigation, it was found that increasing the louver angle (θ), leads to raise the pressure drop and heat transfer. Moreover, the best-performed louver angle was 28 °, while the appropriate range was between 20 °-32 °.

Lee et al. [26] numerically predicted the performance of the louvered fin radiator with flat tube in the range of $100 < Re_{lp} < 3000$. The result discovered that with increasing Re_{lp}, the j and f-factors as well as temperatures (fin surface and exit air) were reduced. Erbay et al. [27] numerically studied twelve 2-D geometries with range of louver angles 20 °-32 ° in a Reynolds number (Re) between 223 and 573. From the investigation, it has been reported that the highest performance was found at Re = 229 and louver angle of 20 °. Moreover, the research disclosed that a greater pressure drop occurred near the edges of the louver. Hosseini et al. [28] investigated

that the air particles tend to deposit on the front and the fin edges of the compact heat exchanger. Such deposition of particles resulted in a larger pressure drop. The impact of ultrasonic excitation on an LFCHE was experimentally investigated and found to improve heat transfer by 70.11% at low air flow velocity and ambient temperature [29]. Okbaz et al. [30] experimentally studied the louvered and wavy finned heat exchangers. The researcher reported that for all of the assessed cases, the *j* and *f*-factors of the louvered finned heat exchangers were higher than the wavy finned heat exchangers. The experimental result revealed the *jf*-factor of the louver fin was higher by 9.6–4.1, 22.1–16, and 16.8–7.4% as compared with the wavy fin for the conditions of two, three, and four tube arrays, respectively. The impacts of louver fin angle, fin pitch, and tube pitch on heat transfer performance and friction factor over a louver angle range of (0 ° to 80 °) were numerically investigated by Ref. [31]. An optimal louver angle of 20 ° was found to maximize Colburn factor and minimize friction factor. Factors were found independent of fin pitch and decreased with the increase in tube pitch. The air side performance of tapered, airfoil, and rectangular LFCHE was numerically studied, with different louver angles and lengths [32]. The highest Nusselt number and minimum friction factor were achieved with the airfoil design, particularly at a louver angle of 23 °.

Based on the existing literature, it has been seen that the LFCHE has better heat dissipation performance than the other fins except for the pressure drop penalty. As the heat transfer increases, the pressure drop increases almost three to four times. Moreover, it has been proved that greater pressure drop occurred on the airside near the edges of the louver. Taking into account the aforementioned problem, this paper is aimed to numerically study the effects of new novel louver edges on the performance of the base model LFCHE using Ansys fluent software. The air side performances of the new louver edges are compared with the existed louver edge under different louver angles and flow conditions. This investigation will serve as a basis for the inevitable design of future radiators and other heat transfer systems. Moreover, it could help in better understanding of the pressure drop and heat dissipation performance on various louver fin edges.

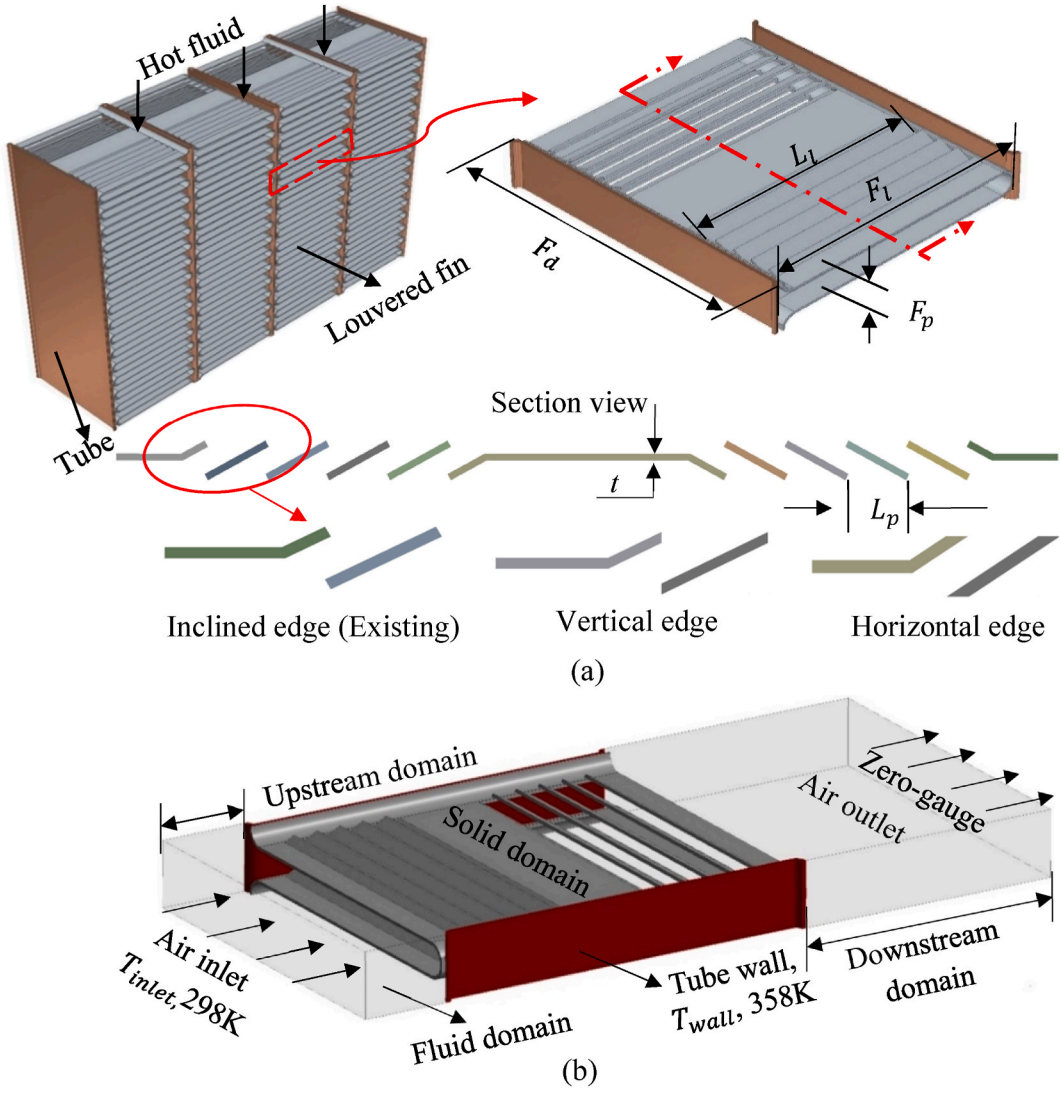

Fig. 1. The overview of the (a) louvered fin geometry with parameters and (b) computational domain with boundary conditions.

2. Model descriptions

2.1. Physical model

A vehicle radiator is made up of a lot of fins and few additional tubes. The overall 3-D model of a radiator generally requires a large number of discrete grids, which increases the computational cost.

Since most of heat exchanger core and flow of air are periodic, one fin pitch and one tube pitch are taken as a computational domain. The developed geometry with its parameters is presented in Fig. 1 (a). The radiator chosen to validate and determine the effect of the louver edges is one of the models that was investigated by Refs. [13,14,26]. The geometric dimensional values of the parameters are presented in Table 1. Since the coolant temperature from the engine reaches around 80–95 °C, the temperature of the coolant is considered as a wall constant temperature (T_{wall}) of 358K at the inner side wall. To mimic the actual test environment, a temperature of 298 K was set for the intake air and the pressure was assumed as zero-gauge pressure.

2.2. Computational domain with boundary conditions

The computational domain is segmented into two regions, as fluid domain and solid (tube and fin) domain, as could be seen in Fig. 1 (b). To maintain uniform inlet air velocity and to ensure that there is no recirculation of air, the length of the upstream and the downstream regions are kept four and ten times the fin pitch, respectively as described in Refs. [24,33].

2.3. Governing equation

To govern the flow of fluid through the domain, conservation of mass, momentum and energy are used based on (Eq. (1)-Eq. (3)) [34]. However, to simplify the analysis and the computational time, the fluid flow is assumed as incompressible and the radiation effect is neglected. A pressure-based solver is used for computation. Among several turbulence models, the Realizable k-ε enhanced wall function turbulence model is used. k is the turbulence of kinetic energy and ε is the rate of kinetic energy dissipation. This wall function has least sensitivity to y+ (dimensionless distance from the wall) values. When the enhanced wall treatment model is employed, the non-dimensional variable is taken as Y+≤ 3. Actually, the value of Y+ is around unity. For solving more accurately the wall viscous sublayer and wall heat transfer of the three-dimensional flow, this model revealed positive results with low-cost running time. The governing equations for this model is given from Eq. (4) to Eq. (6) [34].

Conservation of mass equation:

$$\frac{\partial}{\partial x_i}(\rho u_i) = 0 \tag{1}$$

Momentum equation:

$$\frac{\partial}{\partial x_i}\left(\rho u_i u_j - \tau_{ij}\right) = \frac{\partial p}{\partial x_j} + S_{ij} \tag{2}$$

Where, τ_{ij} is the viscous stress tensor:

$$\tau_{ij} = 2\mu S_{ij} - \frac{2}{3}\mu\frac{\partial u_k}{\partial x_k}\delta_{ij}, S_{ij} = \frac{1}{2}\left(\frac{\partial u_i}{\partial x_j} + \frac{\partial u_j}{\partial x_i}\right)$$

Energy equation:

$$\frac{\partial}{\partial x_i}\left(\rho u_i h - \lambda\frac{\partial p}{\partial x_i}\right) = u_i\frac{\partial p}{\partial x_i} + \tau_{ij}\frac{\partial u_i}{\partial x_i} \tag{3}$$

Realizable k-ε turbulence model:

$$\frac{\partial}{\partial x_i}(\rho k u_i) = \frac{\partial}{\partial x_j}\left(\left(\mu + \frac{\mu_t}{\sigma_k}\right)\frac{\partial k}{\partial x_j}\right) + G_k - \rho\varepsilon - Y_M + S_k \tag{4}$$

$$\frac{\partial}{\partial x_j}(\rho\varepsilon u_i) = \frac{\partial}{\partial x_j}\left(\left(\mu + \frac{\mu_t}{\sigma_\varepsilon}\right)\frac{\partial \varepsilon}{\partial x_j}\right) + \rho C_1 S_\varepsilon - \rho C_2\frac{\varepsilon^2}{k + \sqrt{v\varepsilon}} + S_\varepsilon \tag{5}$$

Table 1
The louver fin radiator base model geometric parameters [13,14,26].

Geometric parameters	Value	Geometric parameters	Value
Fin length, F_l	19 mm	Fin thickness, t	0.16 mm
Fin depth, F_d	22 mm	Tube pitch, T_p	24 mm
Louver length, L_l	17.0 mm	Fin pitch, F_p	1.8 mm
louvered angle, θ	28 °	Tube Thickness	0.61 mm

where, $C_1 = max\left[0.43, \frac{\eta}{\eta+5}\right], \eta = S\frac{k}{\varepsilon}$ and $S = \sqrt{2S_{ij}S_{ij}}$.

The G_k and Y_M indicates the turbulence kinetic energy generation as a result of mean velocity gradients and the fluctuating dilatation contribution to the overall dissipation rate, respectively. C_2 is constant which is 1.9, σ_k is turbulent kinetic energy Prandtl number constant which is 1 and σ_ε is turbulent dissipation rate Prandtl numbers constant which is 1.2. While S_k and S_ε are user-defined source terms.

The eddy viscosity μ_t is turbulent viscosity and computed using Eq. (6).

$$\mu_t = \frac{\rho C_\mu k^2}{\varepsilon} \tag{6}$$

The coupling of pressure and velocity is obtained by utilizing the Coupled scheme and the scheme of second-order upwind discretization is utilized for the momentum and energy equations. The convergence criterion of residual is settled as 10^{-6} for all equations. To perform the required simulation task, Core i9-10850K CPU @ 3.6 GHz, 3600 MHz,10 core(s), 20 logical processors with 32 GB RAM, and 16 GB GPU computer is used.

2.4. Numerical approaches

The pressure drops (Δp) which is the difference in total pressure between the inlet and outlet of the fluid domain and exit air temperature (T_{outlet}) are computed numerically. The data reduction is necessary to determine the airside heat transfer coefficient (h) and is calculated using Log Mean Temperature Difference (LMTD) method as shown in Eq. (7) to Eq. (9).

$$h = \frac{Q}{A_t \Delta T_{lm}} \tag{7}$$

The rate of heat transfer (Q) on the airside is determined as

$$Q = c_p \dot{m}(T_{outlet} - T_{inlet}) \tag{8}$$

The LMTD is calculated as;

$$\Delta T_{lm} = \frac{(T_{wall} - T_{inlet}) - (T_{wall} - T_{outlet})}{\ln[(T_{wall} - T_{inlet})/(T_{wall} - T_{outlet})]} \tag{9}$$

Where; $A_t, \dot{m}, c_p, T_{wall}, T_{inlet}$, and T_{outlet} are the entire area of heat transfer, mass flow rate, specific heat at a constant pressure of air, wall temperature of tube, inlet air temperature, and outlet air temperature, respectively.

The j, f and volume goodness (jf) factor as a function of Re_{lp} are commonly taken as thermal performance evaluation criteria (PEC) and obtained using Eq. (10) to Eq. (13). To get the optimum performance of LFCHE, the condition that the maximum heat transfer (j-factor) with minimum pressure drop (f-factor) must be satisfied. The jf -factor indicates the performance of heat exchanger geometry since it reflects the combined effect of j and f results. If this jf-factor is relatively high, it means that the device requires less volume with the same power consumption for fanning. The jf -factor is calculated using Eq. (13) based on [35,36].

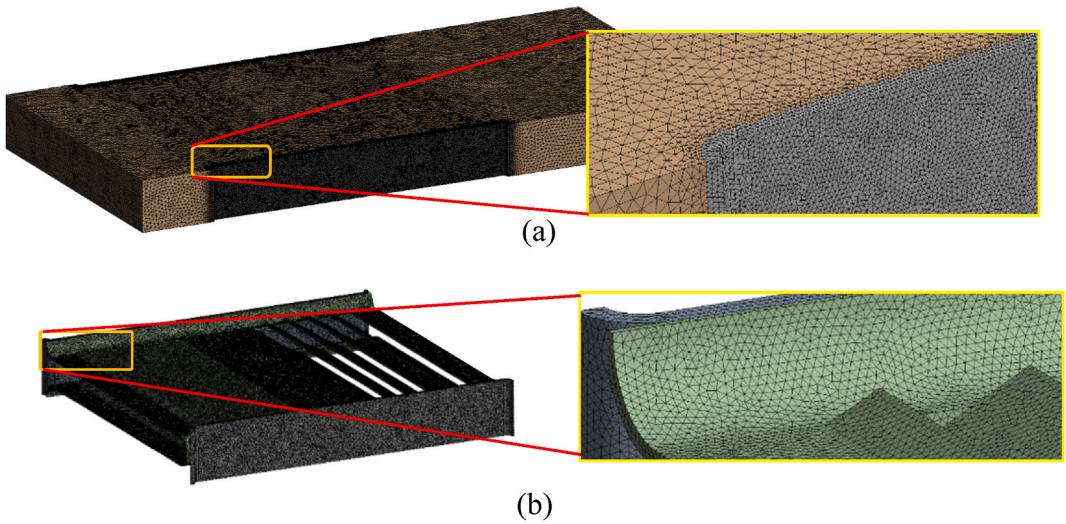

Fig. 2. Computational mesh of (a) fluid domain and (b) solid domain.

$$R_{eLp} = \frac{\rho u L_p}{\mu} \quad (10)$$

$$j - \text{factor} = St * Pr^{2/3} = \frac{h}{\rho_a u_{ava} C_{p,a}} \left(\frac{C_{p,a} \mu_a}{k} \right)^{2/3} \quad (11)$$

$$f = \frac{\Delta P}{\frac{1}{2} \rho_a {u_{ava}}^2} * \frac{A_c}{A_t} \quad (12)$$

$$jf = \frac{j}{f^{1/3}} \quad (13)$$

2.5. Grid generation and independence assessment

The 3D grid system of the computational fluid domain is generated by tetrahedral meshes and the surface mesh is also used for the solid domain to effectively measure the temperature and pressure across the nonslip fin surfaces. The computational mesh for fluid and solid domains are shown in Fig. 2 (a) and Fig. 2 (b), respectively.

To determine the mesh independence of the model, six different grid sizes having numbers of elements are tested (see Table 2). The test result of the pressure drops and the average outlet air temperature at 10 m/s air velocity are presented in Fig. 3 (a) and (b), respectively.

For the last three large numbers of elements around (2.5, 6.5, and 11 million), the pressure-drop and outlet air temperature become almost the same with the average percentile deviation of 0.035%, 0.101%, 0.135% and 0.0323%, 0.01%, 0.024%, respectively. Since the main goal is reducing the number of elements while maintaining the accuracy of the result, a mesh size with around 6.5 million elements is used. Moreover, the iteration is performed up to 500, as no change can be observed beyond that.

2.6. Validation of the numerical method

To verify the validity of the base model, the results of *j* and *f*-factor as a function of Re_{lp} are compared with the previous work of researchers [13,14,26], where the intake air velocity ranges from 1 m/s to 30 m/s. The validation of the current numerical model with other previous research results using similar geometry (presented in Table 1) was performed and shown in Fig. 4. Fig. 4 (a) demonstrates the validation of the numerical model using *j*-factor versus Reynolds number and the associated maximum deviation of 6.5% is recorded at $Re_{lp} = 572$. Fig. 4 (b) shows the validation in terms of friction *f*-factor versus Reynolds number and a maximum deviation of 10% is found at $Re_{lp} = 1450$. Since the deviation is in the permissible range, the model is trustworthy and reliable. Therefore, the model could be used for investigation of the effect of louver edges on the performance of LFCHE.

3. Result and discussion

In this section, the air-side performance of LFCHE with vertical, inclined and horizontal louver edges is investigated. A total of twelve models are formed with the equivalent louver angles (θ) of 20 °, 24 ° , 28 °, and 32 °, and simulated with air velocity ranges from 1 m/s - 30 m/s as shown in Table 3. The numerical results are presented in the form of the area weighted pressure drop and outlet air temperature.

3.1. Louver edge effect

The pressure and temperature distribution of the base model (inclined edge) are presented in Fig. 5 (a) and (b), respectively. Both pressure and temperature distributions on the air side of the fin are investigated at upstream air velocities of 1, 10 and 30 m/s. The result shows that the pressure drop for the geometry increases sharply with increasing inlet velocity (see Fig. 5 (a)). The main reason for this is that as the velocity of the fluid increases, the collisions between the molecules increase and more kinetic energy is lost, which in turn results in a higher pressure drop.

On the other hand, it could be seen in Fig. 5 (b), that the T_{outlet} (downstream temperature) of the air decreases as the velocity of the

Table 2
Mesh size with the number of elements.

Fluid domain mesh size (mm)	Surface mesh size (mm)	Number of elements
0.5	0.5	147,418
0.5	0.25	340,431
0.25	0.25	906,415
0.25	0.15	2,519,590
0.25	0.1	6,523,299
0.25	0.08	11,036,709

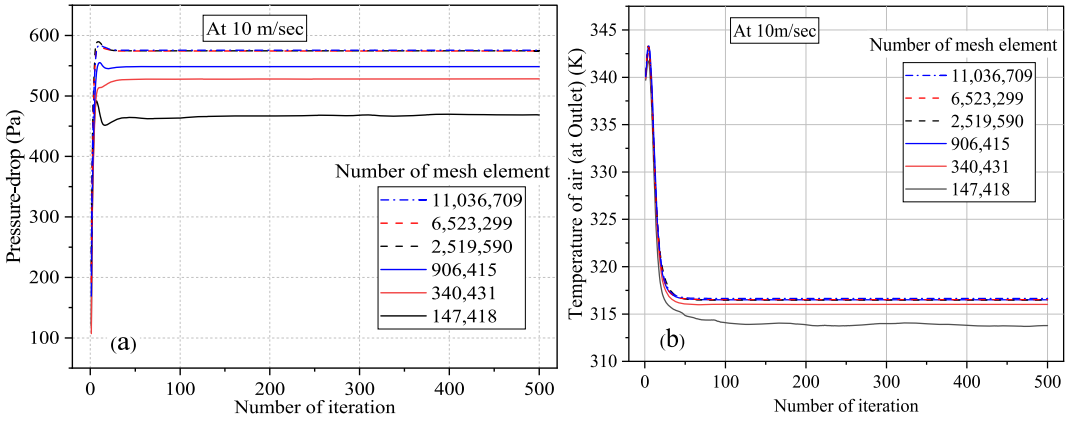

Fig. 3. Mesh independence test (a) pressure drop and (b) Outlet temperature of air.

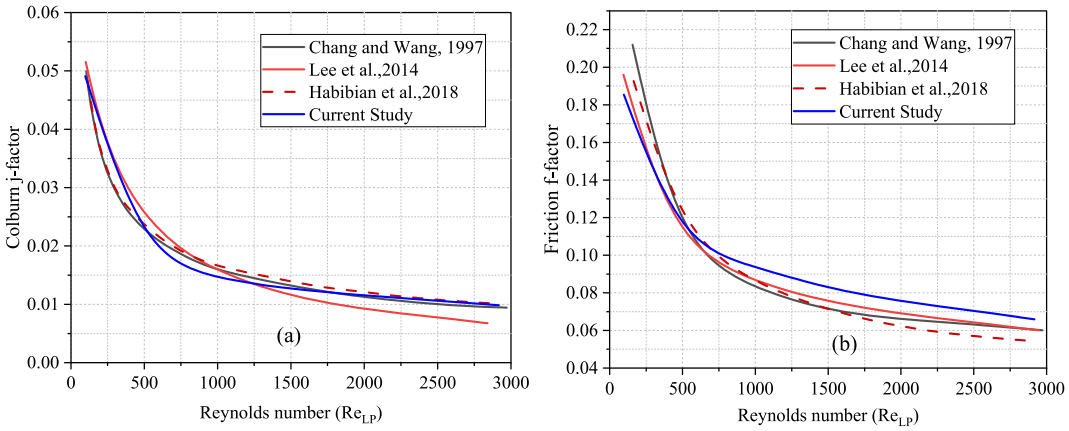

Fig. 4. Numerical model validation (a) Colburn *j*-factor and (b) friction factor.

Table 3
Investigated computational model.

Louver angle (θ)	Edge shape	Air inlet velocity (m/sec)
20 °	Vertical, Inclined Horizontal	1–30
24 °		
28 °		
32 °		

air increases. The fundamental reason for this is that the increase in the mass of the fluid's flow is significantly higher than the increase in the temperature difference between the surface of the fin and the fluid. In addition, the dwell time of the air around the fin decreases with increasing flow velocity, which leads to a lower heat transfer. The two investigations show that the change in temperature is less influenced by the air velocity than by the pressure drops. This result is in agreement with the research finding disclosed by Habibian et al. [14] and Lee et al. [26].

The pressure drops and T_{outlet} for the LFCHE with inclined edge (IE), vertical edge (VE), and horizontal edge (HE) at a base louver angle and with the inlet velocity ranging 1–30 m/s are shown in Fig. 6. The results show that the horizontally edged LFCHE significantly decreased the pressure drop and the vertically edged fins slightly increase on pressure drop of the air side through the fluid domain when compared to the base model (IE fin) in the inlet velocity range considered.

The reason behind is that the shape of the horizontally edged fin behaves as a streamlined flow separation of the air (like a good streamlined body) which reduces the formation of eddy motion or wake as the air flows through the edged louver fin and more air flows through the domain at the same time. However, VE and IE behave like blunt bodies, see Fig. 7. The pressure drops distributions for IE, VE, and HE heat exchangers have been simulated and are presented in Fig. 7. (a), (b), and (c), respectively. The maximum pressure drop increment and decrement were 2.73% and 24.21% from the base louver edge of the blade at 10 m/s for VE and HE, respectively. Moreover, the horizontally edged louvered fin increases the T_{outlet} to 1.01% over the IE louver edges. This is because the

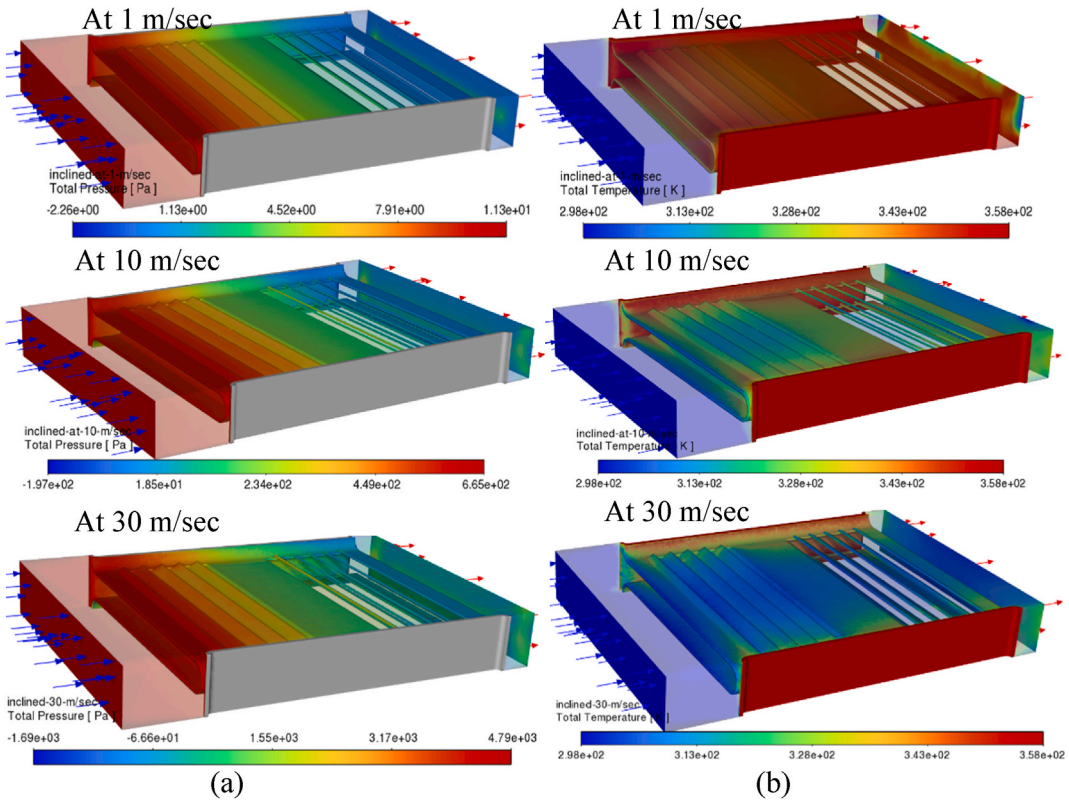

Fig. 5. Pressure (a) and Temperature (b) distribution for inclined edge (base model) at different air inlet velocities.

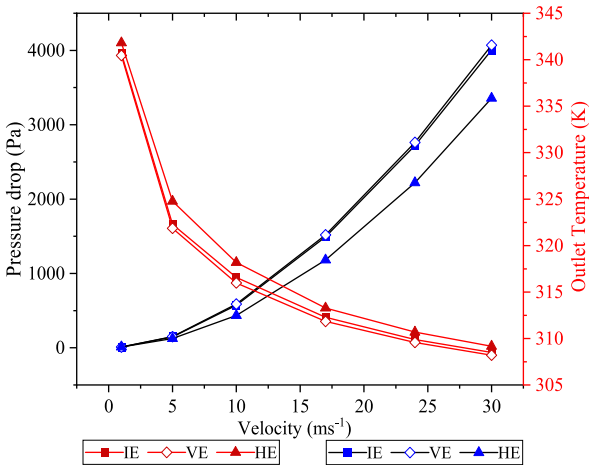

Fig. 6. Pressure drop and outlet air temperature with varied inlet air velocity for different louvered edge shapes.

HE can easily reduce the thickness of boundary layer and enhance the transfer of heat from fin surface to air. Generally, the improved horizontal edge not only increases the heat transfer, but also effectively lowers the pressure drops in a wide range flow condition.

The effects of IE, VE and HE at different louver angles (θ) on the pressure drop and the outlet air temperature are presented in Fig. 8 using numerical simulation. Fig. 8 (a), (b), (c), and (d) demonstrate the respective results of the investigation at air inlet velocities of 1 m/s, 10 m/s, 17 m/s and 30 m/s. The results revealed that the pressure drop increases radically with the inlet velocity as the angle θ increases. This is because the flow separation is forms on the downstream side when the air velocity increases and this increases the pressure drop penalty.

As it could be seen from Fig. 8, the pressure drop for horizontal edged LFCHE is lower than both vertical edge and inclined edge LFCHEs except at very low velocity (1 m/s) for all louver angle (θ). On the other hand, the pressure drop slightly increases for vertical

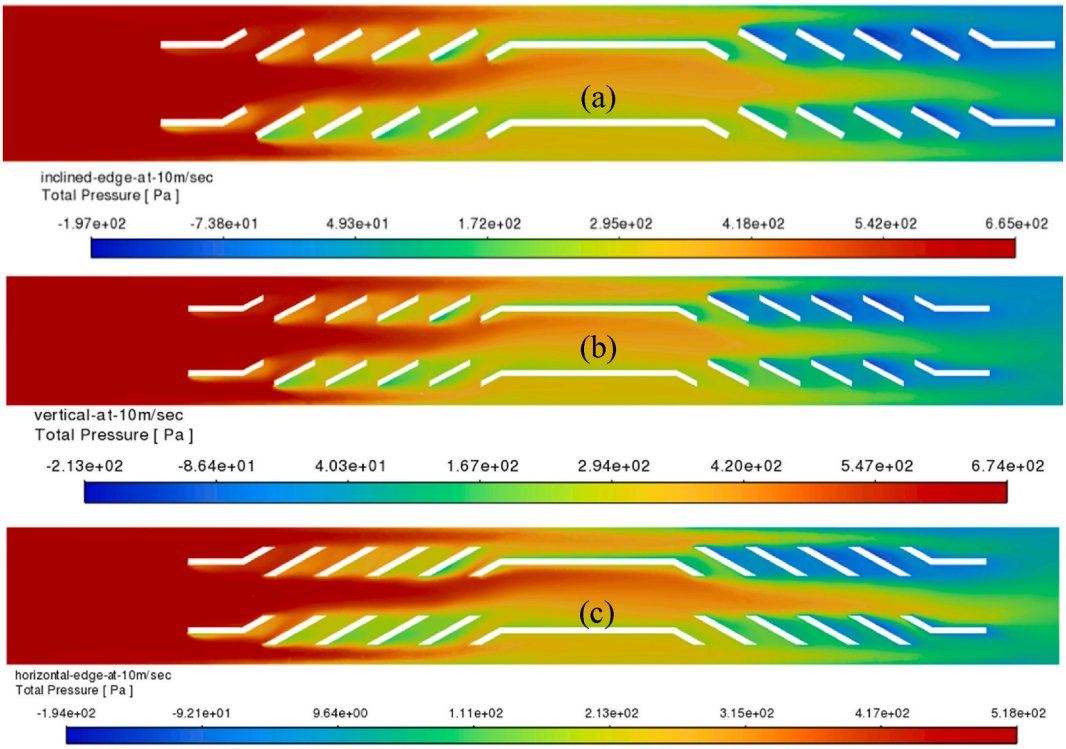

Fig. 7. 2-D pressure distribution of different louver edges; (a) inclined edge (b) vertical edge (c) horizontal edge at 10m/s.

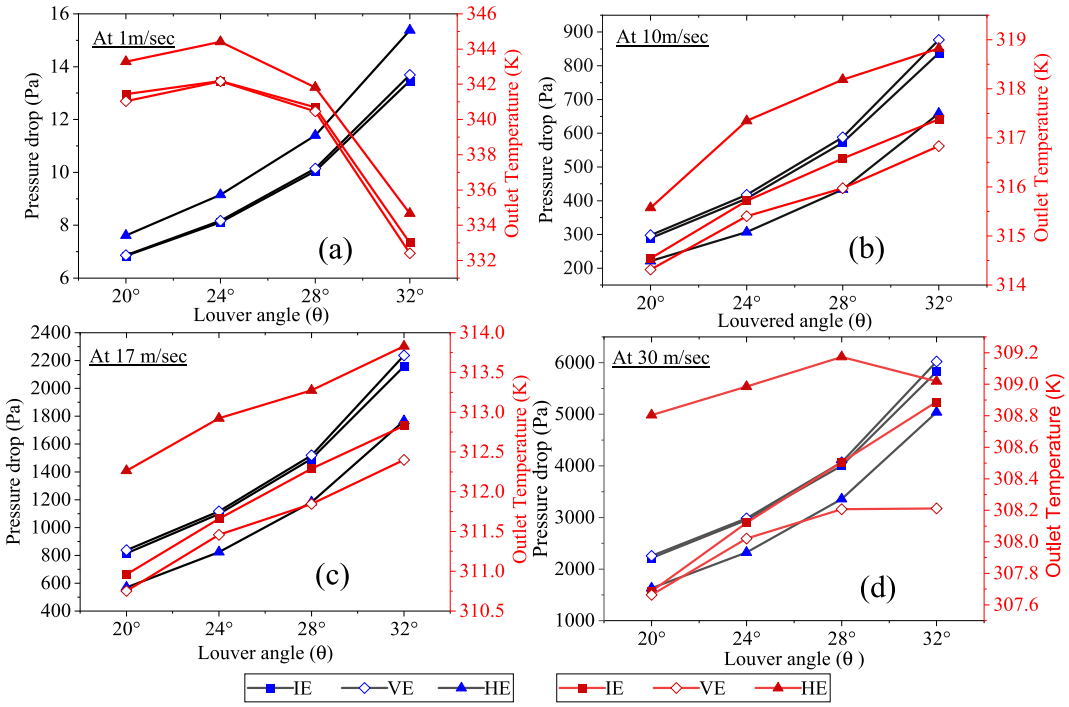

Fig. 8. Pressure drops and outlet temperature of air versus louvered angle for HE, VE, and IE at inlet air velocities of (a), 1 m/s, (b) 10 m/s, (c) 17 m/s, and (d) 30 m/s.

edged LFCHE as compared with the base model. It could also be observed from Fig. 8 (a), (b), (c), and (d) that the outlet air temperature becomes less sensitive to the velocity of air as compared with pressure drop. The simulation result showed that outlet air temperatures for horizontal edge are higher as compared with other two edges (vertical and inclined) for all velocity and louver angles considered. From this, it is plainly observed that even at different louver angles and flow conditions, the horizontal edge improves the transfer of heat as well as helpfully reduces the pressure drop.

3.2. Performance evaluation results of different louver edges

The effects of edges at an angle of 28 ° are illustrated using Performance Evaluation Criteria *j*, *f* and *jf* -factors versus Re_{lp} and presented in Fig. 9 (a), (b), and (c), respectively. The result shows that as Re_{lp} increases, all three factors decrease in the same trend for all edges.

With increasing in Re_{lp}, the fraction of inertial and viscous forces of the flowing fluid increases. Consequently, the particles of the fluid have a greater propensity to keep flowing and are then less affected by viscous braking forces. Ultimately, the *f*-factor reduces as the Re_{lp} increases. This is because, the temperature of the air decreases, resulting in a decrement in air viscosity, which reduces the friction. Moreover, the horizontal edge LFCHE lead an effective increase in *j* and decrease *f*-factor in all Reynolds ranges when compared with the base model. In contrast, the VE decreased in *j* and increased in *f*-factor. The large increment in *j*-factor for horizontally edged was recorded at Re_{lp} of 486.2 and 972.3 by 14.55% and 10.95% over the base edge, respectively. Moreover, the vertically edged revealed a decrement in the *j* by 3.47% at Re_{lp} of 972.3.

The edge effects on volume goodness factor have been investigated at different air inlet velocities and louvered angles. The volume goodness factor versus louvered angle of the three edges at inlet air velocities of 1 m/s, 10 m/s, 17 m/s, and 30 m/s are presented in Fig. 10 (a), (b), (c), and (d), respectively. The results of the edge effect are presented in terms of the *jf*-factor, as this factor integrates *j* and *f*. The results show that the HE has a high value of *jf*-factor in all flow conditions. Compared to the base model, the *jf*-factor for horizontal edged LFCHE at 10 m/s ($Re_{lp} = 972.3$) increased by 21.5%. In contrast, the *jf*-factor for vertically edged LFCHE decreased by 4.65% as compared with the base model. This indicates that the horizontally edged LFCHE performs well on compromising the heat transfer with pressure drop and requires a minimal volume at the same power for fanning.

As the louver angle increased, *jf*-factor increased for all louver edges, since the *j* and *f* increased as a result of longer flow length. At

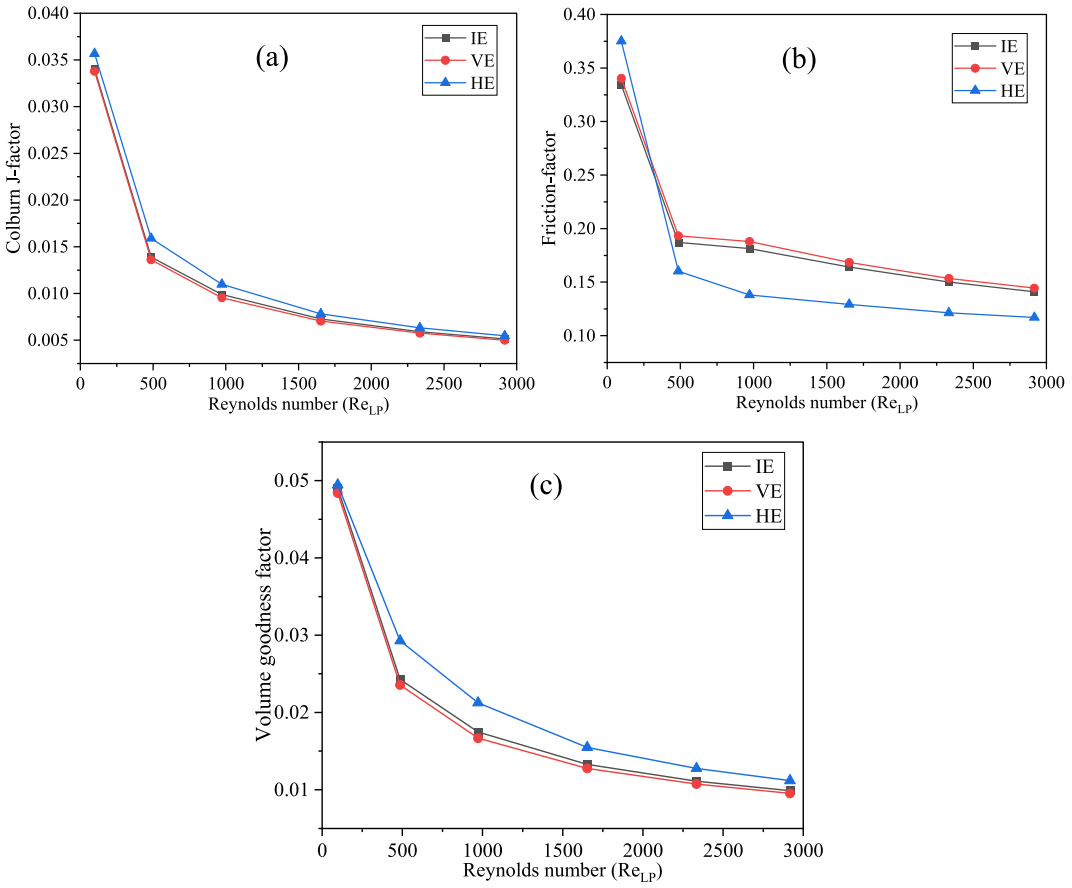

Fig. 9. (a) *j*-factor, (b) *f*-factor, and (c) Volume goodness (*jf*)-factor versus Re_{lp}.

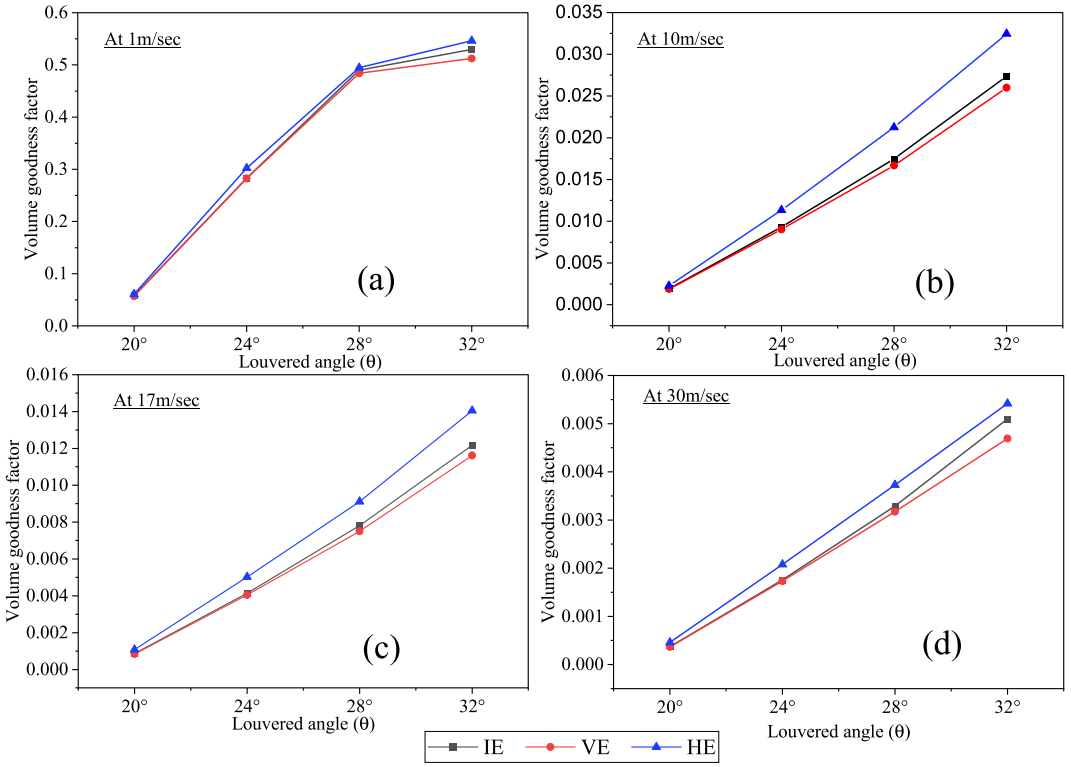

Fig. 10. Volume goodness factor versus different louver angles at inlet air velocities of (a), 1 m/s, (b) 10 m/s, (c) 17 m/s, and (d) 30 m/s.

the velocity of 10 m/s the factor for HE increased by 22.0% and 17.2% at angle θ of 24 ° and 20 °, respectively. However, at a higher air velocity, the horizontal edge increased the performance up to 25.3% at louver angle 20 °, compared with the base louver edge.

4. Conclusion

The louver edges (vertical, inclined, and horizontal) effect on louvered fin compact heat exchanger performance with differing louver angle (θ) and flow conditions were numerically investigated. The numerical investigation on the effects of vertical and horizontal edges has been done in the comparison with the base model (inclined edge). From the numerical investigation, the following conclusions are drawn:

- When louver pitch-based Reynolds number increases, the *j*, *f* and *jf*-factor decrease for all louver edges. For the Re_{lp} range from 97 to 2917, the horizontal edge increased the *jf*-factor up to 21% when compared with the base model. Based on the three performance evaluation criteria, horizontally edged louvered fin compact heat exchanger radiator shows highest performance over the other two cases.
- As the louver angle (θ) increases, the *j*, *f* and *jf*-factors also increase for all louver edges and flow conditions. Moreover, for all louver angles, the horizontal edge louvered fin compact heat exchanger achieved higher *jf*-factor. The best louver angle for horizontally edged is 24 ° and 20 ° at low and high Reynolds number, respectively.
- The horizontally edged louvered fin compact heat exchanger significantly decreases the pressure drop as compared with the base model. Whereas, the result showed that the pressure drops for vertical edged heat exchanger slightly higher than the base model. The outlet temperature of air is less affected by different louver edges across the fluid domain as compared to the pressure drop.
- This research is limited to the numerical investigation of three different louver edges. It lacks experimental validation and a more comprehensive geometric analysis. Therefore, future work should consider practical tests with more comprehensive geometric investigation.

Generally, the numerical simulation results revealed that the horizontal edge effectively lowers the pressure drop in a wide variety of flow conditions in addition to slightly improving heat transfer. Hence, horizontal edged LFCHE are more preferred than other two edges. However, it is recommended to the manufacturing and practical aspects.

Data availability statement

Data will be available on request.

CRediT authorship contribution statement

Dessalew Shite Feleke: Writing – original draft, Software, Methodology, Investigation, Funding acquisition, Conceptualization. **Muluken Z. Getie:** Writing – review & editing, Validation, Methodology, Conceptualization. **Temesgen Asefa Minale:** Writing – original draft, Visualization, Methodology, Data curation, Conceptualization.

Declaration of competing interest

The authors of this research declare that we have no competing financial interests or personal relationships that could have appeared to influence the work reported in this research.

Acknowledgments

The investigation was supported by the faculty of Mechanical and Industrial Engineering, Bahir Dar institute of Technology, Bahir Dar University, Ethiopia.

References

[1] K. Ryu, S. Yook, K. Lee, Optimal design of a corrugated louvered fin, Appl. Therm. Eng. 68 (2014) 76–79, https://doi.org/10.1016/j.applthermaleng.2014.04.022.
[2] L.B. Erbay, B. Doğan, M.M. Öztürk, Comprehensive study of of heat exchangers with louvered fins, IntechOpen Sci (2017) 61–92, https://doi.org/10.5772/66472.
[3] Q. Zuoqin, W. Qiang, C. Junlin, D. Jun, Simulation investigation on inlet velocity profile and configuration parameters of louver fin, Appl. Therm. Eng. (2018) 173–182, https://doi.org/10.1016/j.applthermaleng.2018.02.009.
[4] T.K.K. Byeong Kook Yoo, Min Seok Kim, Ye in Bang, Jongwon Kim, Numerical analysis and correlation of thermohydraulic characteristics of louvered fin-tube heat exchanger, Int. J. Refrig. 147 (2023) 121–133, https://doi.org/10.1016/j.ijrefrig.2022.08.021.
[5] A. Sadeghianjahromi, C. Wang, Heat transfer enhancement in fin-and-tube heat exchangers – a review on different mechanisms, Renew. Sustain. Energy Rev. 137 (2021) 110470, https://doi.org/10.1016/j.rser.2020.110470.
[6] A. Sadeghianjahromi, S. Kheradmand, H. Nemati, Developed correlations for heat transfer and flow friction characteristics of louvered finned tube heat exchangers, Int. J. Therm. Sci. 129 (2018) 135–144, https://doi.org/10.1016/j.ijthermalsci.2018.03.002.
[7] K. Javaherdeh, A. Vaisi, R. Moosavi, The effects of fin height, fin-tube contact thickness and Louver length on the performance of a compact fin-and-tube heat exchanger, Int. J. Heat Technol. 36 (2018) 825–834, https://doi.org/10.18280/ijht.360307.
[8] R. Moosavi, A. Vaisi, K. Javaherdeh, Investigation of the geometrical structure of louvered fins in fin-tube heat exchangers for determining the minimum distance of the headers, J. Mech. Sci. Technol. 35 (2021) 1721–1731, https://doi.org/10.1007/s12206-021-0335-4.
[9] H. Fugmann, E. Laurenz, L. Schnabel, Multi-dimensional performance evaluation of heat exchanger surface enhancements, MDPI Energies 12 (2019), https://doi.org/10.3390/en12071406.
[10] C.J. Davenport, Correlations for heat transfer and flow friction characteristics of louvred fin, AIChE Symp. Ser. ser. 79 (1983) 19–27.
[11] T.A. Cowell, M.R. Heikal, U. Kingdom, A. Achaichia, Flow and heat transfer in compact louvered fin surfaces LH-, Exp. Therm. Fluid Sci. 1777 (1995) 192–199.
[12] R.L. Webb, S.H. Jung, Air-side performance of enhanced brazed aluminium heat exchangers, ASHRAE Trans 98 (1992) 1–401.
[13] Y.J. Chang, C.C. Wang, A generalized heat transfer correlation for Iouver fin geometry, Int. J. Heat Mass Tran. 40 (1997) 533–544, https://doi.org/10.1016/0017-9310(96)00116-0.
[14] S.H. Habibian, A. Mostafazade Abolmaali, H. Afshin, Numerical investigation of the effects of fin shape, antifreeze and nanoparticles on the performance of compact finned-tube heat exchangers for automobile radiator, Appl. Therm. Eng. 133 (2018) 248–260, https://doi.org/10.1016/J.APPLTHERMALENG.2018.01.032.
[15] K. Dodiya, N. Bhatt, F. Lai, Louvered fin compact heat exchanger: a comprehensive review, Int. J. Ambient Energy 0 (2020) 1–39, https://doi.org/10.1080/01430750.2020.1839549.
[16] J.M. Gorman, M. Carideo, E.M. Sparrow, J.P. Abraham, Case Studies in Thermal Engineering Heat transfer and pressure drop comparison of louver- and plain-finned heat exchangers where one fluid passes through flattened tubes, Case Stud. Therm. Eng. 5 (2015) 122–126, https://doi.org/10.1016/j.csite.2015.03.002.
[17] M.S. Yadav, S.A. Giri, V.C. Momale, Sizing analysis of louvered fin flat tube compact heat exchanger by genetic algorithm, Appl. Therm. Eng. (2017), https://doi.org/10.1016/j.applthermaleng.2017.07.119.
[18] M. Kim, C.W. Bullard, Air-side thermal hydraulic performance of multi-louvered fin aluminum heat exchangers, Int. J. Refrig. 25 (2002) 390–400.
[19] X. Zhang, D.K. Tafti, Flow efficiency in multi-louvered fins, J. Heat Tran. (2002) 61801.
[20] D.K. Tafti, J. Cui, Fin-tube junction effects on flow and heat transfer in flat tube multilouvered heat exchangers, Int. J. Heat Mass Tran. 46 (2003) 2027–2038, https://doi.org/10.1016/S0017-9310(02)00509-4.
[21] A. Vaisi, M. Esmaeilpour, H. Taherian, Experimental investigation of geometry effects on the performance of a compact louvered heat exchanger, Appl. Therm. Eng. 31 (2011) 3337–3346, https://doi.org/10.1016/j.applthermaleng.2011.06.014.
[22] P.A. Sanders, K.A. Thole, Effects of winglets to augment tube wall heat transfer in louvered fin heat exchangers, Int. J. Heat Mass Tran. 49 (2006) 4058–4069, https://doi.org/10.1016/j.ijheatmasstransfer.2006.03.036.
[23] N. Tran, C. Wang, Optimization of the airside thermal performance of mini-channel-flat-tube radiators by using composite straight-and-louvered fins, Int. J. Heat Mass Tran. 160 (2020) 120163, https://doi.org/10.1016/j.ijheatmasstransfer.2020.120163.
[24] A. Saleem, M.-H. Kim, CFD analysis on the air-side thermal-hydraulic performance of multi-louvered fin heat exchangers at low Reynolds numbers, MDPI Energies 10 (2017), https://doi.org/10.3390/en10060823.
[25] K. Javaherdeh, A. Vaisi, R. Moosavi, M. Esmaeilpour, The experimental and numerical investigations on louvered fin-and-tube heat exchanger with variable geometrical parameters, J. Therm. Sci. Eng. Appl. 9 (2017), https://doi.org/10.1115/1.4035449.
[26] S.H. Lee, N. Hur, S. Kang, An efficient method to predict the heat transfer performance of a louver fin radiator in an automotive power system, J. Mech. Sci. Technol. 28 (2014) 145–155, https://doi.org/10.1007/s12206-013-0951-8.
[27] L.B. Erbay, N. Uğurlubilek, Ö. Altun, B. Doğan, Numerical investigation of the air-side thermal hydraulic performance of a louvered-fin and flat-tube heat exchanger at low Reynolds numbers, Heat Tran. Eng. 38 (2017) 627–640, https://doi.org/10.1080/01457632.2016.1200382.

[28] S.B. Hosseini, R.H. Khoshkhoo, M.J. Pii, Experimental and numerical investigation on particle deposition in a compact heat exchanger, Appl. Therm. Eng. 115 (2017) 406–417, https://doi.org/10.1016/j.applthermaleng.2016.12.110.
[29] A. Amiri Delouei, H. Sajjadi, M. Atashafrooz, M. Hesari, M.B. Ben Hamida, A. Arabkoohsar, Louvered fin-and-flat tube compact heat exchanger under ultrasonic excitation, Fire 6 (2023), https://doi.org/10.3390/fire6010013.
[30] A. Okbaz, A. Pınarbaşı, A.B. Olcay, Experimental investigation of effect of different tube row-numbers, fin pitches and operating conditions on thermal and hydraulic performances of louvered and wavy finned heat exchangers, Int. J. Therm. Sci. 151 (2020), https://doi.org/10.1016/j.ijthermalsci.2019.106256.
[31] A. Sadeghianjahromi, S. Kheradmand, H. Nemati, C.C. Wang, Optimization of the louver fin-and-tube heat exchangers -a parametric approach, J. Enhanc. Heat Transf. 27 (2020) 289–312, https://doi.org/10.1615/JENHHEATTRANSF.2020033527.
[32] X. Zhang, Y. Huang, J. Song, Z. Ma, L. Chen, T. Li, Numerical investigation of the air-side performance of louver fin-and-tube radiators having rectangular, tapered and airfoil section configuration, Energy Rep. 8 (2022) 11799–11809, https://doi.org/10.1016/j.egyr.2022.09.050.
[33] A. Saleem, M. Kim, Airside thermal performance of louvered fin flat-tube heat exchangers with different redirection louvers, MDPI Energies 12 (2022), https://doi.org/10.3390/en15165904.
[34] T.J. Baker, ANSYS FLUENT user ' s guide, Knowl. Creat. Diffus. Util. 15317 (2021) 724–746. https://www.scribd.com/document/501588564/ANSYS-Fluent-Tutorial-Guide-2021-R1.
[35] M. Zeeshan, S.A. Hazarika, S. Nath, D. Bhanja, Numerical investigation on the performance of fin and tube heat exchangers using rectangular vortex generators, AIP Conf. Proc. 1859 (2017), https://doi.org/10.1063/1.4990164.
[36] L.B. Erbay, B. Doğan, M.M. Ozturk, Numerical analysis of thermo-hydraulic performance of flibe flowing through a louvered-fin compact heat exchanger, SSRN Electron. J. 8300 (2022) 1–29, https://doi.org/10.2139/ssrn.4090280.